

# Proceedings of the Institution of Mechanical Engineers, Part D: Journal of Automobile Engineering

<http://pid.sagepub.com/>

---

## Effects of the dimensional and geometrical tolerances on the kinematic and dynamic performances of the Rzeppa ball joint

Pier Paolo Valentini

*Proceedings of the Institution of Mechanical Engineers, Part D: Journal of Automobile Engineering* published online 28 October 2013

DOI: 10.1177/0954407013505745

The online version of this article can be found at:

<http://pid.sagepub.com/content/early/2013/10/28/0954407013505745>

---

Published by:



<http://www.sagepublications.com>

On behalf of:



[Institution of Mechanical Engineers](http://www.institutionofmechanicalengineers.org)

---

Additional services and information for *Proceedings of the Institution of Mechanical Engineers, Part D: Journal of Automobile Engineering* can be found at:

**Email Alerts:** <http://pid.sagepub.com/cgi/alerts>

**Subscriptions:** <http://pid.sagepub.com/subscriptions>

**Reprints:** <http://www.sagepub.com/journalsReprints.nav>


**Permissions:** <http://www.sagepub.com/journalsPermissions.nav>

>> [OnlineFirst Version of Record](#) - Oct 28, 2013

[What is This?](#)

# Effects of the dimensional and geometrical tolerances on the kinematic and dynamic performances of the Rzeppa ball joint

Pier Paolo Valentini

Proc IMechE Part D:  
J Automobile Engineering  
0(0) 1–13  
© IMechE 2013  
Reprints and permissions:  
sagepub.co.uk/journalsPermissions.nav  
DOI: 10.1177/0954407013505745  
pid.sagepub.com  


## Abstract

In this paper the influences of some relevant dimensional and geometrical errors on both the kinematic performance and the dynamic performance of an automotive Rzeppa ball joint were investigated. The study focused on the development of a dedicated and improved multi-body three-dimensional model of the joint and the corresponding numerical simulations of different configurations. The model is able to manage the presence of the redundant constraints which are present in the joint architecture because of the use of spring connections between parts which replace most of the kinematic constraints or geometrical contact conditions. Three types of error were investigated, and both kinematic irregularities and dynamic irregularities are reported in graphs and discussed. The effects of different articulation angles between the inner ring and the outer ring were also investigated.

## Keywords

Rzeppa joint, tolerance, multi-body dynamics, discrete flexible multi-body, mechanical error

Date received: 27 March 2013; accepted: 22 August 2013

## Introduction

Coupling joints are widely used in mechanical and industrial applications in order to transmit torque and motion between two misaligned or displaced shafts.<sup>1</sup> Among all the relevant features that a designer requires in a coupling joint, two are the most important: constant-velocity (homokinetic) transmission and load capacity.<sup>2</sup> The homokinetic condition is fulfilled when the angular velocity of the input shaft is always equal to that of the output shaft, irrespective of the angular misalignment (articulation angle  $\beta$ ) and irrespective of the rotation angle.<sup>3</sup> On the other hand, the load capacity is related to the capability of transferring an adequate amount of torque between the two shafts without failure, irregularities or vibration sources.

Among the variety of coupling joints, the Rzeppa typologies (designed and patented by the inventor Alfred Hans Rzeppa) gained a relevant role in the last century. Their use began in 1936 in front-wheel-drive passenger cars produced in the USA. Their distinctive capability is to transmit torque between inclined shafts ideally at a constant velocity. In fact, there are a variety of different structures with different geometrical

features but almost the same functioning principle. The variants have been used in applications such as aircraft, marine and industrial stationary drive systems.

One of the most common Rzeppa joint structures (F2 classification according to Seherr-Thoss et al.<sup>1</sup>) consists of an inner ring, an outer ring, a cage and a series of balls (Figure 1).

Each ring has a series of meridian grooves in which the balls are constrained to move. In the most widespread automotive implementation, the central lines of the grooves are planar circumferences belonging to planes which are inclined at a constant angle  $\gamma$  with respect to the axis of the joint (Figure 1(b)). Moreover, the centres of the balls are constrained to be located in a plane by the presence of a metallic cage. The condition of homokineticity, which will be discussed in detail

---

Department of Enterprise Engineering, University of Rome 'Tor Vergata', Rome, Italy

### Corresponding author:

Pier Paolo Valentini, Department of Enterprise Engineering, University of Rome 'Tor Vergata', Via del Politecnico, I-00133 Rome, Italy.  
Email: valentini@ing.uniroma2.it

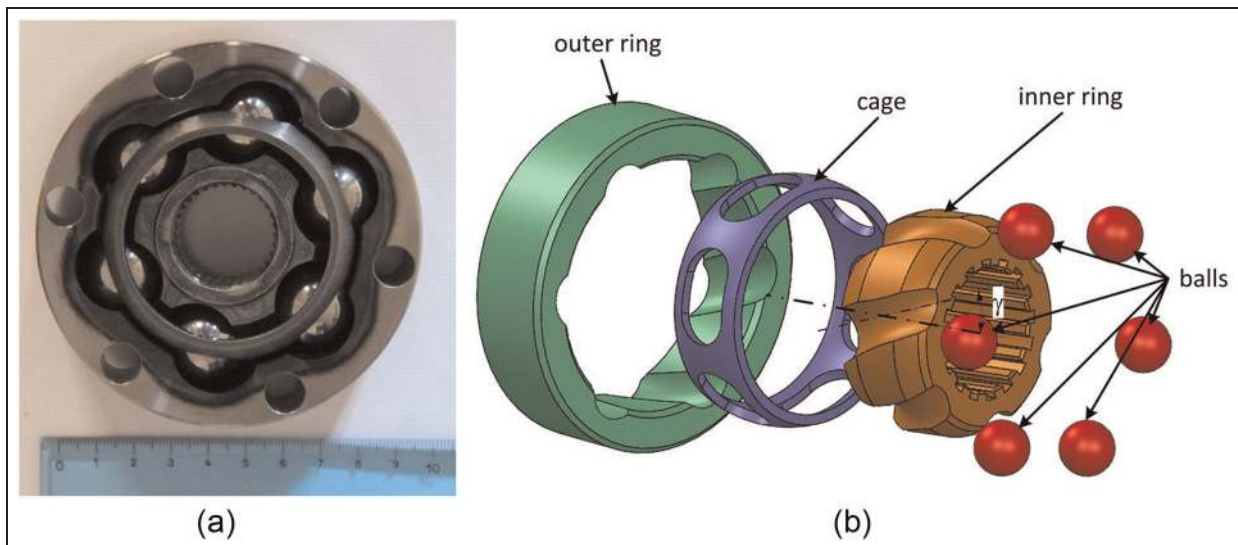


**Figure 1.** (a) Photograph of an automotive Rzeppa ball joint; (b) schematic diagram of the computer-aided design model.

in the next section of the paper, is due to the precise shape and to the assembled features that fulfil geometrical and kinematic considerations.

In practical applications, because of the presence of limited manufacturing precision and assembling errors, some irregularities may be present in the device operation. These variations may alter the kinematic performance of the joint, producing a variable speed ratio between the input shaft and the output shaft and causing the homokineticity of the coupling to vanish. Moreover, irregularities may cause variations in the reaction forces of the internal constraints, contacts and mounting supports. Compliance and elasticity of the parts also introduce other possible causes of irregularities. An accurate and comprehensive design should take into account all these complications by trying to prevent or control them. A study on the influence of the errors and the compliance effects in the mechanisms is fundamental for an accurate design and a specific allocation of the tolerances in manufacturing, as testified by several contributions in different fields (see, for example, the papers by Brutti et al.,<sup>4</sup> Pezzuti et al.<sup>5</sup> and Valentini<sup>6</sup>).

Numerical models have been widely used for addressing the investigations in many fields of mechanical transmissions. On the other hand, most of the papers on coupling joints have dealt with ideal conditions. Next we consider the contributions in very recent years relating to the constant-velocity joints. In 2001, Hayama<sup>7</sup> presented an ADAMS model for assessing the internal forces of a double-offset constant-velocity universal joint, neglecting the friction contribution. In 2004, Mariot et al.<sup>8</sup> developed a kinetostatic model including friction in order to simulate the behaviour of both tripod joints and ball joints. In 2005, Kimata et al.<sup>9</sup> discussed a dynamic three-dimensional (3D) model of a ball joint, estimating the contact forces between the parts. In 2008, Serveto et al.<sup>10</sup> investigated the

influence of the geometry and the friction on the secondary torque of an automotive drive shaft. In 2008, Pennestrì et al.<sup>11</sup> performed a kinematic and dynamic analysis of a special type of non-homokinetic Rzeppa joint (the so-called pilot-lever joint). More recently, in 2009, Lim et al.<sup>12</sup> discussed a very interesting model of a complete transmission, including tripod joints and Rzeppa joints.

Papers dealing with the modelling and simulation of joints with geometrical and dimensional tolerances are limited. The most relevant problem for these investigations is that, in general, a numerical model suitable for the simulation of an ideal joint is not suitable for the description of imprecisions and compliances but requires a more specialized adaptation. In a simple joint, the kinematic loop equations may be altered in order to introduce errors and the simulation of the behaviour can be performed by using the same dynamic equations as in the ideal case (see, for example, the papers of Fisher and XXX<sup>13</sup> and Valentini and Pezzuti<sup>14</sup>). In a more complex joint, the kinematic equations quite often do not take into account the presence of redundant loops and structural elasticity. In particular, for the Rzeppa solution, a single ball moving inside two grooves and a spherical joint connecting the two shafts may be sufficient to describe the kinematics of the joint.<sup>1</sup> The presence of several ball-groove contacts is required to increase the load capacity and to distribute the transmission forces. On the other hand, the kinematic description of these repetitions produces redundant constraints which are satisfied simultaneously only if ideal conditions are fulfilled. The presence of errors causes this mathematical approach to fail and requires a different simulation strategy. In general, neglecting redundancy and considering a single loop tend to overestimate the kinematic irregularities since, in the real solution, the errors in a single loop are partially dumped and balanced by the



**Figure 2.** Wear due to contact between the ball and the cage in an automotive Rzeppa joint after functioning for 5000 h.

others. In the same way, the contact forces are underestimated because over-abundant reactions are neglected. For this reason, an accurate assessment of the effects of the dimensional and geometrical errors has to take into account the constraint redundancy.

In 2009, Cozzolini et al.<sup>15</sup> presented a multi-body model of the Rzeppa joint (F1 classification according to Seherr-Thoss et al.<sup>1</sup>) for assessing some of the possible errors. This computational model is a good starting point for the investigation, but it has some important simplifications that produced an approximated estimation of the influences of the errors. First of all, the Cozzolini et al. model did not take into account the effect of the metallic cage. This can be an important limitation, since experimental evidence (Figure 2) shows that the contact forces between the balls and the cage are relevant and produce local deformation (and wear). Moreover, the model made use of massless points to describe the ball–groove connections, which made the model numerically unstable for high-speed and high-load transmission.

For all these reasons, the purpose of the present study is to discuss a 3D model of a Rzeppa joint, which is suitable for generic investigations of the influences of the elasticity and the dimensional and geometrical errors on its performance.

The paper is organized as follows. First, the functional and geometrical details of the investigated Rzeppa joint typology are presented. Second, the implementation of the model is discussed, focusing on the description of contact elements. Third, the results of some simulations including the presence of relevant errors are presented and discussed.

## Morphology and functionality of the Rzeppa joint

The investigated solution of the Rzeppa joint consists of an inner ring, an outer ring, a cage and six balls (see Figure 1). Each ring has six meridian grooves, obtained with toroidal pockets. The medial curves (in general,

circumferences) of these grooves have centres located at the centre of the joint, and they are contained in planes which are misaligned at a constant angle  $\gamma$  (positive for the inner ring and negative for the outer ring) with respect to the axis of the corresponding ring. This geometrical feature ensures the positioning of the centres of the balls at the intersections between the corresponding medial curves pairs. These intersections are contained in a plane (transmission plane) which passes also for the intersection of the inner shaft and outer shaft axes. Moreover, because of the specific geometrical design, it can be demonstrated<sup>1</sup> that the transmission plane is coincident with the homokinetic plane irrespective of the articulation angle between the input shaft and the output shaft (Figure 3).

In fact, in order to preserve the condition of homokineticity, all the centres of the balls must be located in the bisector plane with respect to the axes of the input shaft and the output shaft according to the theorem stated by Myard.<sup>16</sup> This geometrical locus, which represents the kinematic plane of transmission, is often called the homokinetic plane.

When the shafts are misaligned, the ball–groove contacts cause the centre of each ball to lie at the intersection of the two corresponding medial circumferences of the grooves. Because of the specific geometry, the intersections belong to the homokinetic plane for every misalignment angle. In all the practical implementations, a metallic cage is added to enforce all the ball centres to be constrained to a single plane.

## Mathematical model of the Rzeppa joint

The proposed mathematical model of the Rzeppa joint is constructed using multi-body dynamics techniques, by considering all the bodies as rigid and including concentrated elastic elements in order to simulate the effects of structural compliance and contacts (Figure 4). This approach allows kinematic joint redundancies to be avoided and the distributed reaction forces to be computed. Of course, this approach requires a specific assessment of the position and the properties of the elastic elements in order to preserve the actual kinematic and compliance characteristics. Moreover, changing the kinematic constraints into penalty constraints allows the geometrical and dimensional errors to be introduced more easily and avoids producing a system with redundant equations.

### Modelling of contacts

By observing the actual configuration of the joint, it can be seen that the mechanical actions between the balls and the grooves originated from contact mechanics. Under ideal conditions and neglecting deformations, each groove geometry constrains the ball centre so that it belongs to its medial circumference. With this consideration, each ball was modelled with two equivalent balls of the same radius but half the



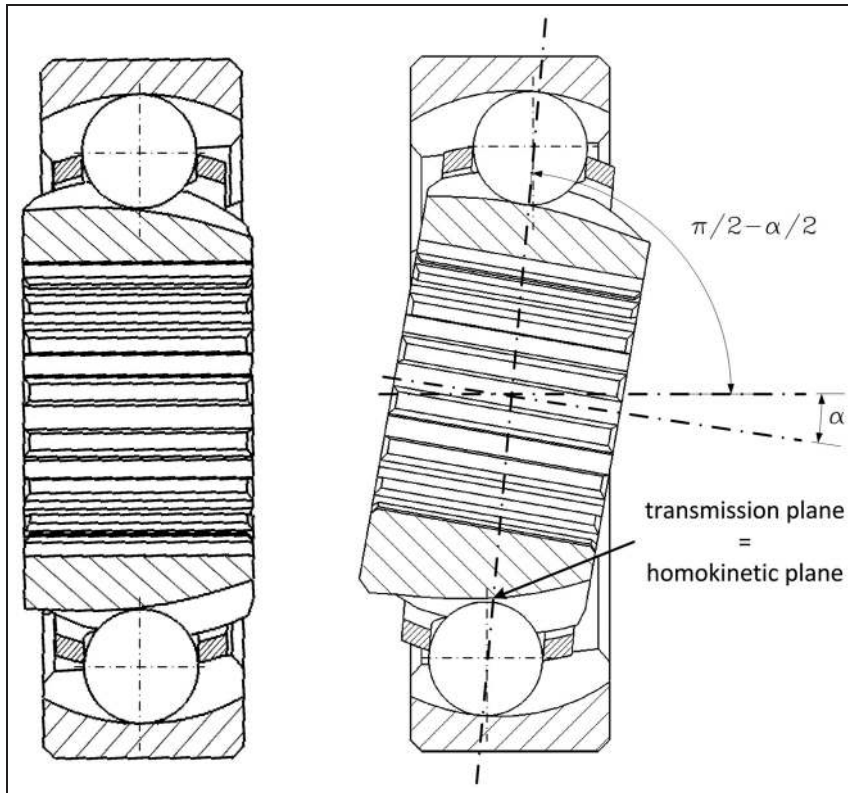


Figure 3. Kinematic articulation of the inner ring and the cage in order to obtain a homokinetic transmission.

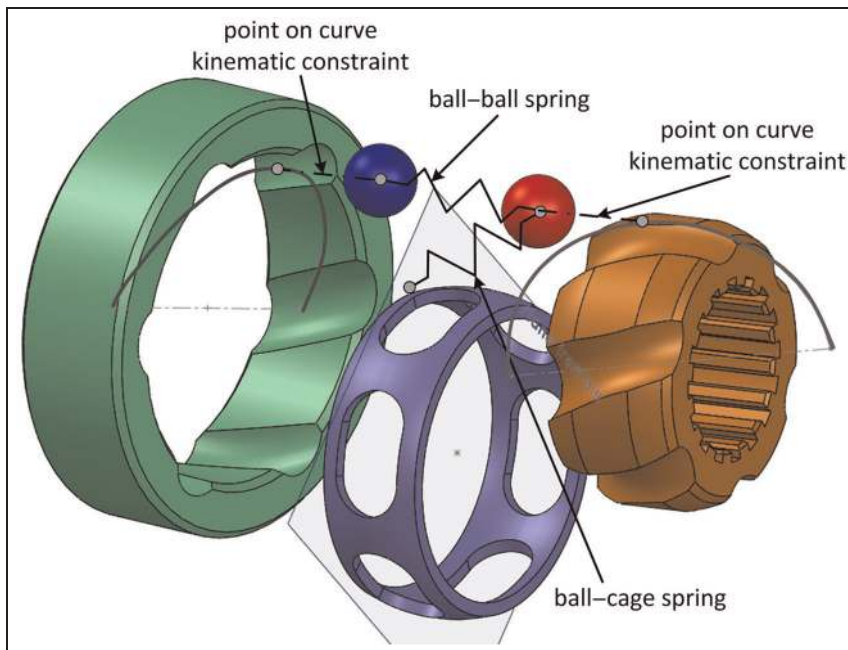


Figure 4. Kinematic constraints and elastic springs for simulating the contact mechanics between bodies and avoiding kinematic redundancies.

mass density. The centre of the first equivalent ball was constrained to be coincident with the meridian circumference of the inner-ring groove. In the same way, the centre of the second equivalent ball was constrained to be coincident with the meridian circumference of the

outer-ring groove. A two-degree-of-freedom point-to-curve kinematic constraint was imposed on both these connections and this constraint is given by

$$C_j - P_{j,k}(u) = 0 \tag{1}$$

where  $C_j$  is the centre of the  $j$ th ball and  $P_{j,k}(u) = \{x(u) \ y(u) \ z(u)\}^T$  is the parametric expression ( $u$  is the parameter) of the  $j$ th meridian curve on the  $k$ th ring. The constraints in equation (1) leave free four degrees of freedom, namely three rotations and a translation along the curve, described by the parameter  $u$ .

In order to connect the two corresponding balls, an equivalent spring was linked between their two centres. This link forces the two equivalent balls to be coincident, restoring the main functionality of the joint, but allows the compliance needed to avoid an over-constrained system of equations. From a physical point of view, the spring simulates the contact stiffness between the balls and the grooves which the kinematic constraint in equation (1) is not able to take into account.

The elastic characteristics of the equivalent springs are computed from the Hertz contact theory using the formulae in Roark's atlas.<sup>17</sup> Following this approach, the force–displacement relationship for a sphere–groove contact can be computed using the expression

$$y = \lambda \sqrt[3]{\frac{F^2 C_E^2}{K_D}} \quad (2)$$

where  $F$  is the applied compression force,  $y$  is the displacement (the variation in the distance between the centre of the ball and the groove),  $C_E$  is a constant depending on the material properties of the bodies in contact,  $K_D$  is a constant depending on the geometrical curvatures of the bodies where the contact occurs and  $\lambda$  is a coefficient depending on the misalignment between the principal curvature directions of the two bodies. Considering the symmetry of the ball, it can be assumed that  $\lambda = 0.288$ ; considering both the balls and the rings to be made of the same material,  $C_E$  can be computed as

$$C_E = 2 \frac{1 - \nu^2}{E} \quad (3)$$

where  $E$  is Young's modulus and  $\nu$  is Poisson's ratio.

The cross-section of the grooves is in general elliptical or ogival. Considering the minimum radius of curvature of the cross-section to be almost equal to the radius of the balls, the coefficient  $K_D$  can be approximated as<sup>17</sup>

$$K_D = \frac{1.5}{1/R_{ball} + 1/R_{groove}} \quad (4)$$

where  $R_{ball}$  is the radius of the ball and  $R_{groove}$  is the radius of the inner meridian circumference of the groove.

In fact, the direction of the force in the ball–groove contact depends on the pressure angle  $\alpha$  of the assembly. For this reason, the displacement  $y_{ball-ball}$  of the spring has to be projected on the contact line in order to deduce the actual penetration distance  $y$  (Figure 5); thus,

$$y_{ball-ball} = \frac{y}{\sin \alpha} \quad (5)$$

Moreover, a ball is in contact with the two grooves of both the inner ring and the outer ring, and so the contact compliance is doubled. For this reason, the corrected relationship between the force and the displacement to be assigned to the elastic element connecting the two balls is

$$y_{ball-ball} = \frac{2}{\sin \alpha} \lambda \sqrt[3]{\frac{F^2 C_E^2}{K_D}} \quad (6)$$

where  $y_{ball-ball}$  is the distance between the centres of the spheres.

In order to describe the contact between the balls and the cage, another series of elastic elements was included. Since the faces of the cage which are in contact to the balls are planar, we can consider these elements connecting the centres of the balls as the midplane of the cage, with springs whose stiffness can

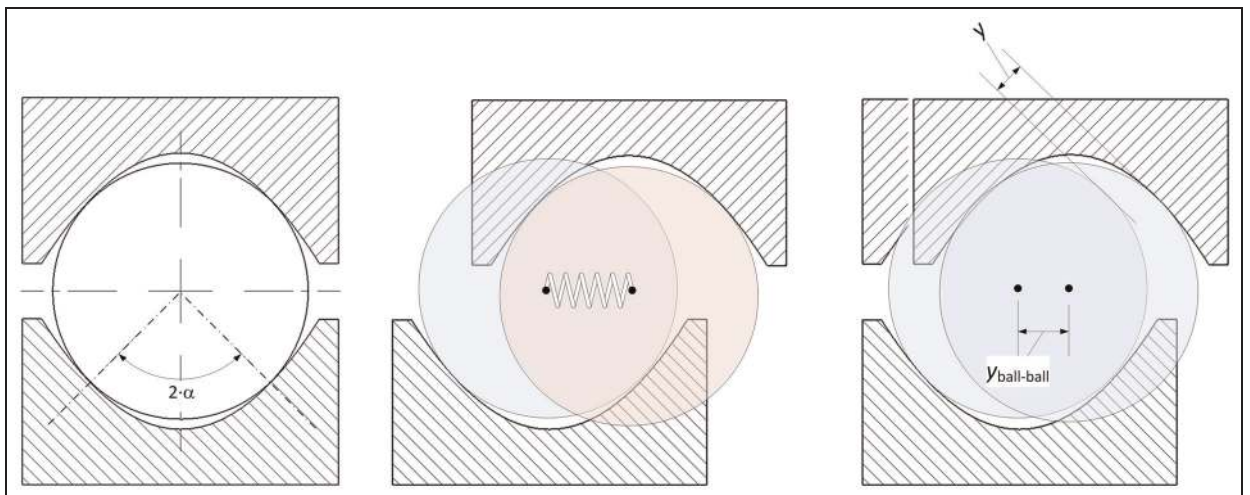


Figure 5. Geometrical relationship between the spring displacement and the contact penetration.

be computed using another relationship based on the Hertz contact theory<sup>14</sup> and given by

$$y_{ball-cage} = \lambda \sqrt[3]{\frac{F^2 C_E^2}{K_D}} \quad (7)$$

where  $y_{ball-cage}$  is the distance between the centre of the ball and the cage midplane,  $K_D = 2R_{ball}$  and  $\lambda = 1.040$ .

Since the contact between the balls and the cage occurs on only one side at a time, a single spring connecting only one of the two ball pairs is sufficient.

Linear damping characteristics  $c$  were added to all the springs. They simulate the structural contact damping of steel and they were considered as 5% of the corresponding critical values approximated by

$$c = 0.05 \times 2 \sqrt{km_{eq}} \quad (8)$$

where  $k$  is the average stiffness value of the element which connect the two parts and  $m_{eq}$  is the equivalent mass of the subsystem (which can be approximated as the mass of the smaller connected part).

Considering that the joint is usually well lubricated (it is sealed and filled with grease), friction has been neglected in each contact pair.

### Other constraints

The model also includes a revolute joint for constraining the inner ring to the ground and a revolute joint for constraining the outer ring to the ground, which leaves free the rotational degrees of freedom around its axis.

A constant rotational velocity (driving constraint) was imposed on the inner ring and a constant resisting torque was applied to the outer ring.

The equations governing the dynamics of each model were implemented, using a Lagrangian approach<sup>18</sup> and managing a redundant set of variables,<sup>19</sup> and were solved using the GSTIFF integrator.<sup>20</sup> The equations of motion were arranged and solved in terms of generalized coordinates according to

$$\frac{d}{dt} \frac{\partial T}{\partial \dot{q}_i} - \frac{\partial T}{\partial q_i} - \frac{\partial \psi^T}{\partial q_i} \cdot \lambda = Q_i \quad \psi = 0 \quad (9)$$

where  $q_i$  is the  $i$ th generalized coordinate ( $i$  goes from 1 to the number of generalized coordinates),  $\dot{q}_i = dq_i/dt$

is the time derivative of the  $i$ th generalized coordinate,  $T$  is the kinetic energy of the system,  $\psi$  is the vector containing the constraint equations written in terms of the generalized coordinates (this term includes the contribution of the prescribed rotation of the inner ring),  $\lambda$  is the vector containing the Lagrange multipliers associated with each constraint and  $Q_i$  is the sum of all generalized forces acting on the  $i$ th coordinate  $q_i$  (this term contains all the contributions of the contact springs and the external torque applied to the outer ring).

### Ideal configuration and errors

The first set of simulations concerns the ideal configuration of the joint, i.e. a joint whose parts do not have any error. The joint was simulated at misalignments of 5°, 10° and 15° in order to investigate also how this influences the performances.

The main geometrical and simulation parameters are reported in Table 1.

Three different errors were investigated. The maximum tolerance values of these errors are chosen according to the ISO 2768-1 recommendation for medium-precision manufacturing.<sup>21</sup>

The first error is a geometrical error of flatness which may occur in the cage geometry. Since the cage forces the balls to belong to a single transmission plane, an error in the flatness influences the fulfilment of this condition. In fact, this error forces the points of contact between the balls and the cage to be offset with respect to the expected contact plane, with the consequence that the centres of the ball will be offset too.

For this reason, the flatness error in the cage was simulated by changing the zero-force length of all the springs which connect the cage to the ball centres. The values of these zero-force lengths were chosen by picking random variations in the interval  $\pm 0.2$  mm, as suggested by the ISO norm for the flatness error.

The second simulated error is a dimensional inaccuracy concerning the radius of one of the medial circumference of the grooves of the inner ring. According to the ISO 2768-1 recommendation for medium-precision manufacturing, the amplitude of the above-mentioned error was assumed to be 0.3 mm. It was included by directly changing the geometrical parameter which

**Table 1.** Geometrical (without errors) and simulation parameters of the numerical investigations.

Parameter	Value
Radius $R_{groove}$ of the radius of the inner meridian circumference of the groove	45 mm
Inclination $\gamma$ of the inner-ring groove and outer-ring groove with respect to their axes	10°
Radius $R_{ball}$ of the ball	10 mm
Young's modulus $E$ of the material of each part	206 GPa
Poisson's ratio $\nu$ of the material of each part	0.3
Rotational velocity $\omega_{in}$ of the inner ring	1000 r/min
Resisting torque $T$ of the outer ring	50 N m

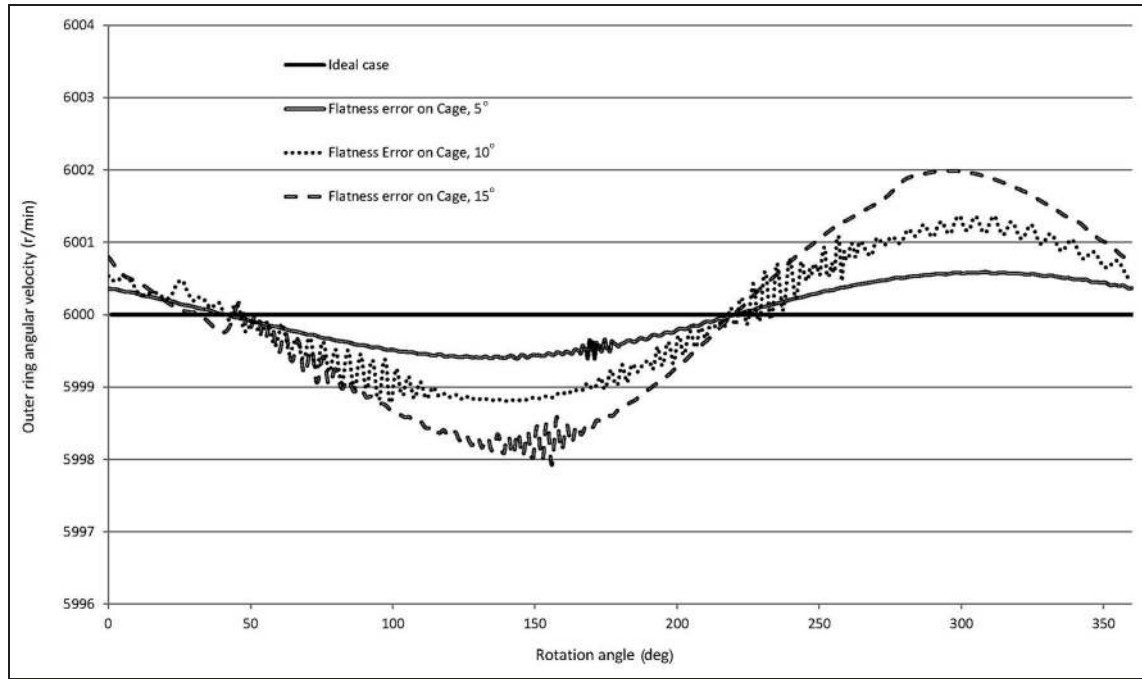


**Figure 6.** Kinematic irregularities in the angular velocity of the outer ring due to the flatness error of the cage.

defines the radius of one medial circumference of the groove.

The third simulated error is an angular misalignment of the inclination of the plane in which one of the inner-groove meridian circles is located. According to the ISO 2768-1 recommendation for medium-precision manufacturing, the amplitude of the error was assumed to be  $0.5^\circ$ . Again, it was included by directly changing the geometrical parameter which defines the inclination of the plane in which one of the inner-groove meridian circles is located.

### Simulation approach

In order to assess the influences of the investigated errors on the kinematic and dynamic performances of the Rzeppa joint, several characteristics were monitored. These are the rotational speed of the outer ring (which gives an assessment of the kinematic irregularities) and the reaction forces and moments of both revolute joints between the rings and the ground (which give an assessment of the dynamic irregularities).

In the ideal case (i.e. perfect geometry), the transmission ratio is constant and the angular velocity of the outer ring is also constant. The reaction forces and moments on the revolute joints of both the inner ring and the outer ring are also constant because they need to balance the well-known secondary torque  $C_2$  arising from the global equilibrium of the system,<sup>10</sup> which is given by

$$C_2 = C_{in} \tan\left(\frac{\vartheta}{2}\right) \quad (10)$$

where  $C_{in}$  is the input torque and  $\vartheta$  is the angle of misalignment (i.e. the articulation angle).

In the case of errors, a variation in the constant values is expected.

### Results and discussion

Starting with the first error, the geometrical inaccuracy in the flatness of the cage causes the loss of perfect homokineticity with irregularities in the transmission ratio with the same frequency as that of the rotation (Figure 6). The higher-frequency oscillations in the graphs are due to numerical errors in the integration of the equations which, however, do not cause instability, and so they can be neglected. The irregularities increase almost linearly with increasing articulation angle. At  $15^\circ$ , they reach a maximum of 0.3%.

The reaction forces and moments acting on the revolute joints of both the inner ring and the outer ring are also irregular but with a frequency which is the double that of the rotation. Figures 7 and 8 present these irregularities for the inner ring. It can be observed that the mean value of the dynamic actions is almost the same as that of the ideal case, while the amplitudes of the irregularities increase with increasing misalignment angle between the inner ring and the outer ring. The higher-frequency oscillations in the graphs are due to numerical errors in the integration of the equations which, however, do not cause instability. The irregularities in and the amplitudes of the outer ring are very similar, and their graphs are omitted.

Concerning the second error, the dimensional inaccuracy in the radius of one of the meridian grooves of the inner ring causes the loss of perfect homokineticity



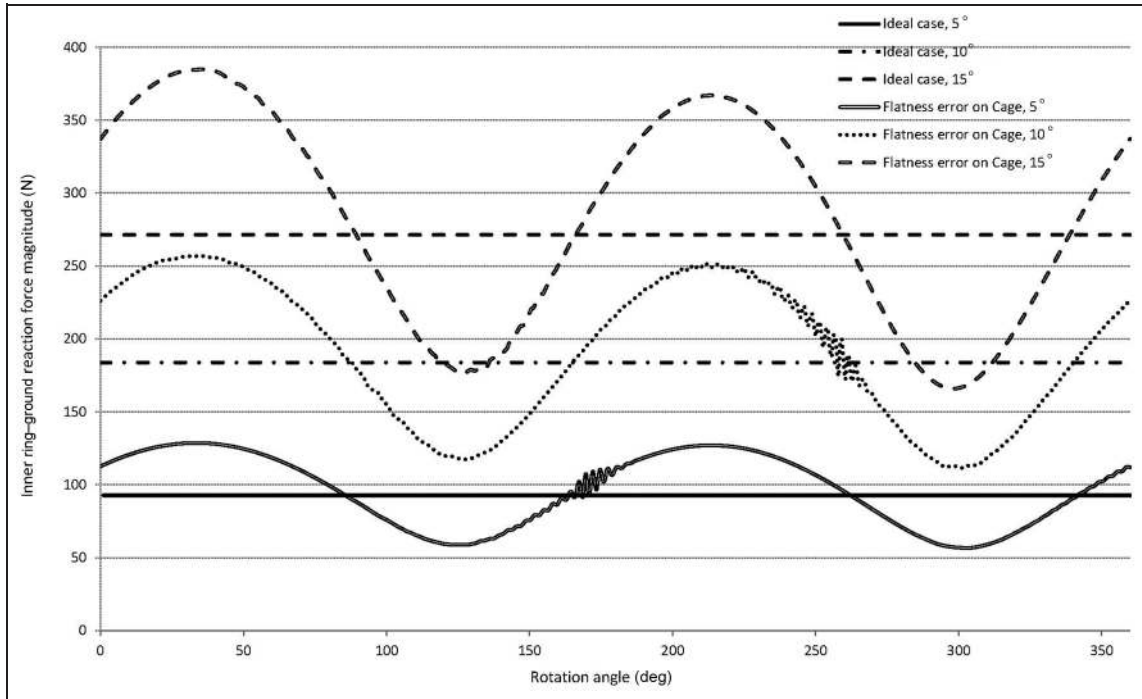


Figure 7. Dynamic irregularities in the inner-ring-ground reaction force due to the flatness error of the cage.

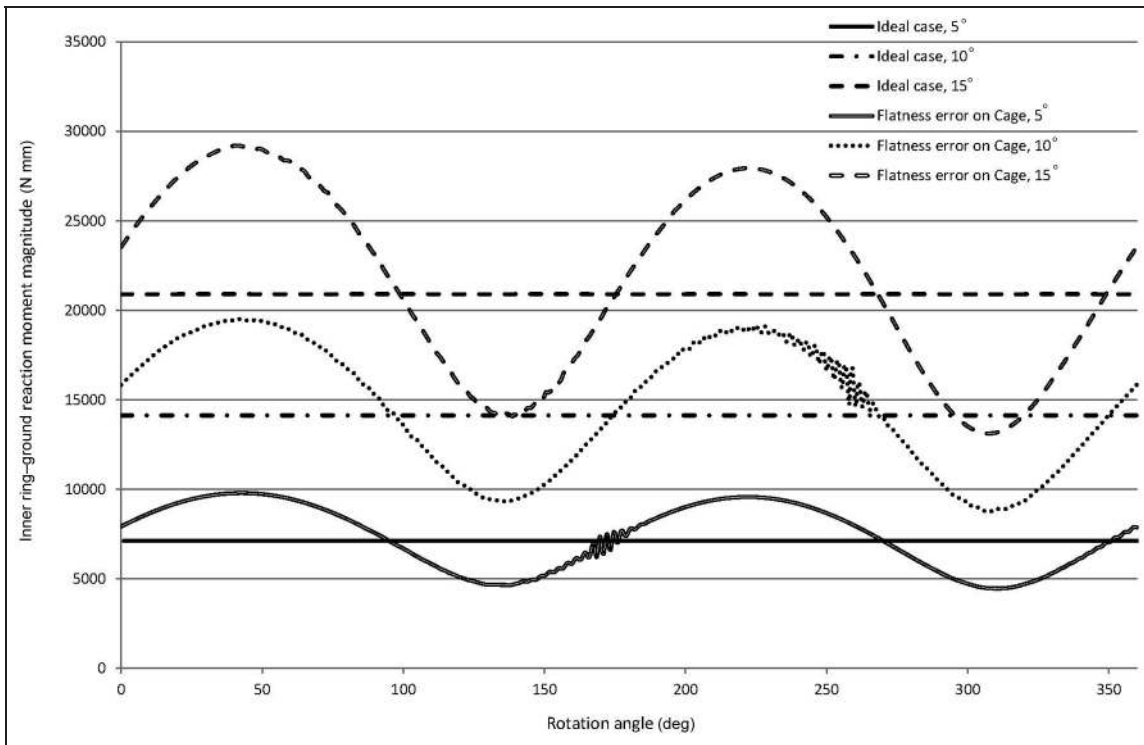
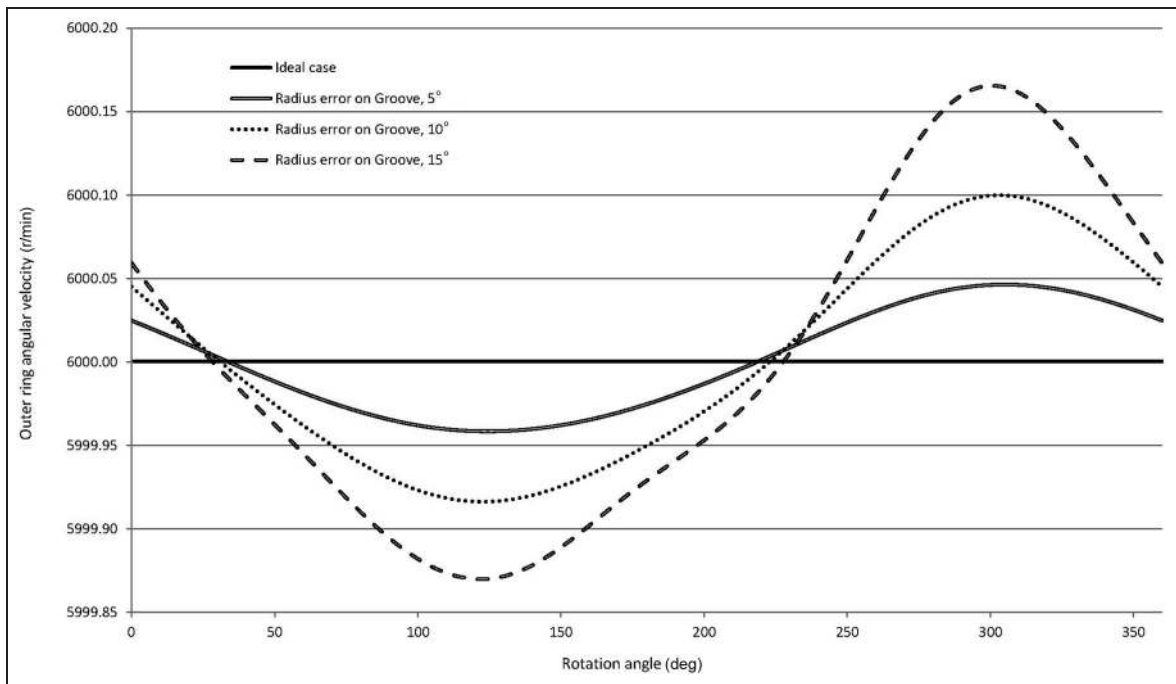


Figure 8. Dynamic irregularities in the inner-ring-ground reaction moment due to the flatness error of the cage.

with irregularities in the transmission ratio with the same frequency as that of the rotation (Figure 9). The amplitudes of these irregularities are much smaller than those caused by the first error. They increase with increasing

articulation angle between the inner ring and the outer ring. At 15°, they reach a maximum of  $2.1 \times 10^{-3}\%$ .

The reaction forces and moments acting on the revolute joints of both the inner ring and the outer ring are



**Figure 9.** Kinematic irregularities in the angular velocity of the outer ring due to the dimensional error in the radius of the inner-ring groove.

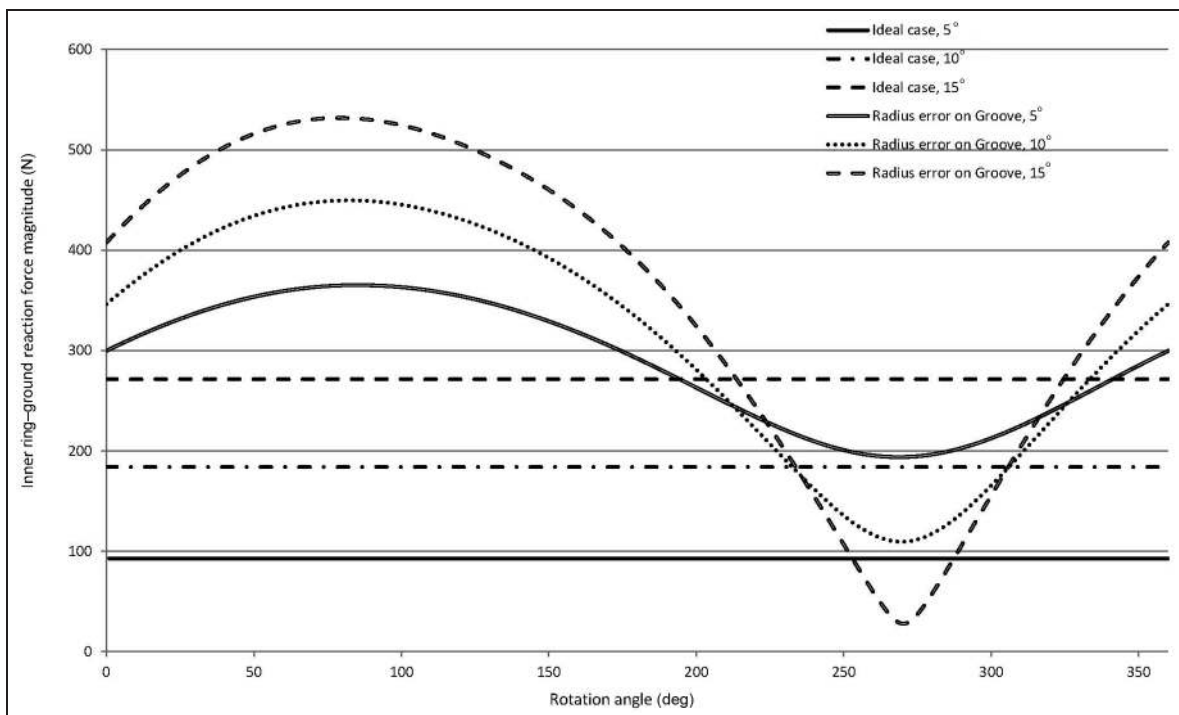


**Figure 10.** Dynamic irregularities in the inner ring-ground reaction force due to the dimensional error in the radius of the inner-ring groove.

also irregular with a frequency which is the same as that of the rotation. Figures 10 and 11 present these irregularities on the inner ring. It can be observed that the mean value of the dynamic action is different from the ideal case and that their amplitudes increase with increasing articulation angle between the inner ring and

the outer ring. The irregularities in and the amplitudes of the outer ring are very similar, and again their graphs are omitted.

Concerning the third error, the angular inaccuracy in the plane of the medial circumference of one of the meridian grooves of the inner ring causes the loss of perfect

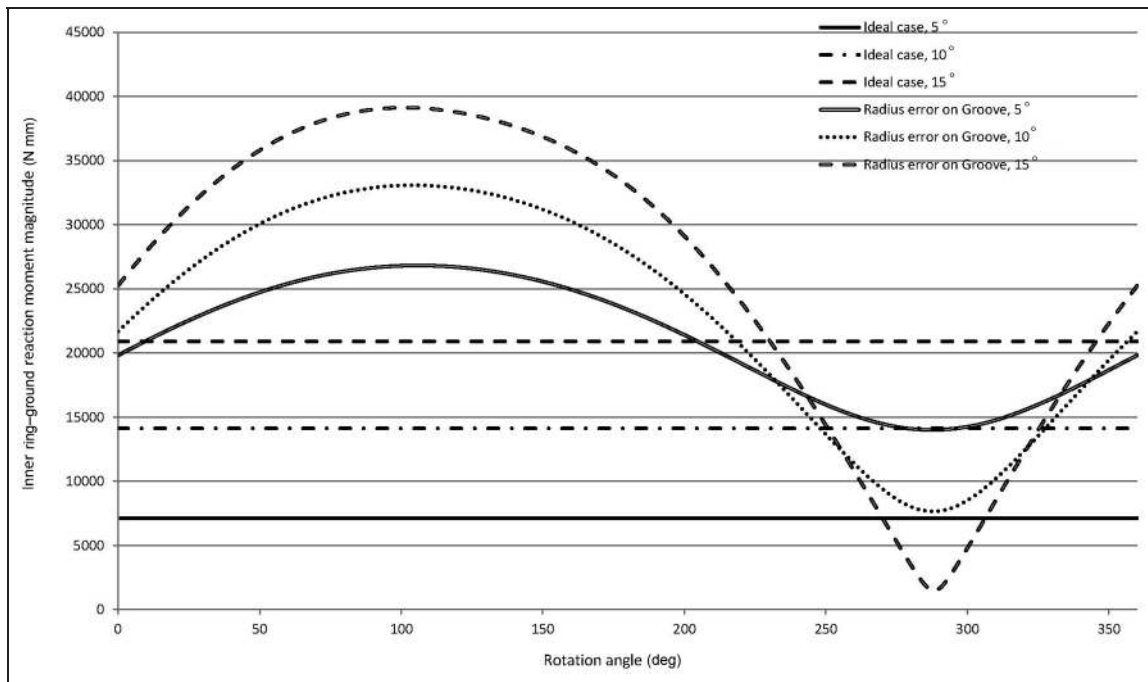


**Figure 11.** Dynamic irregularities in the inner ring-ground reaction moment due to the dimensional error in the radius of the inner-ring groove.

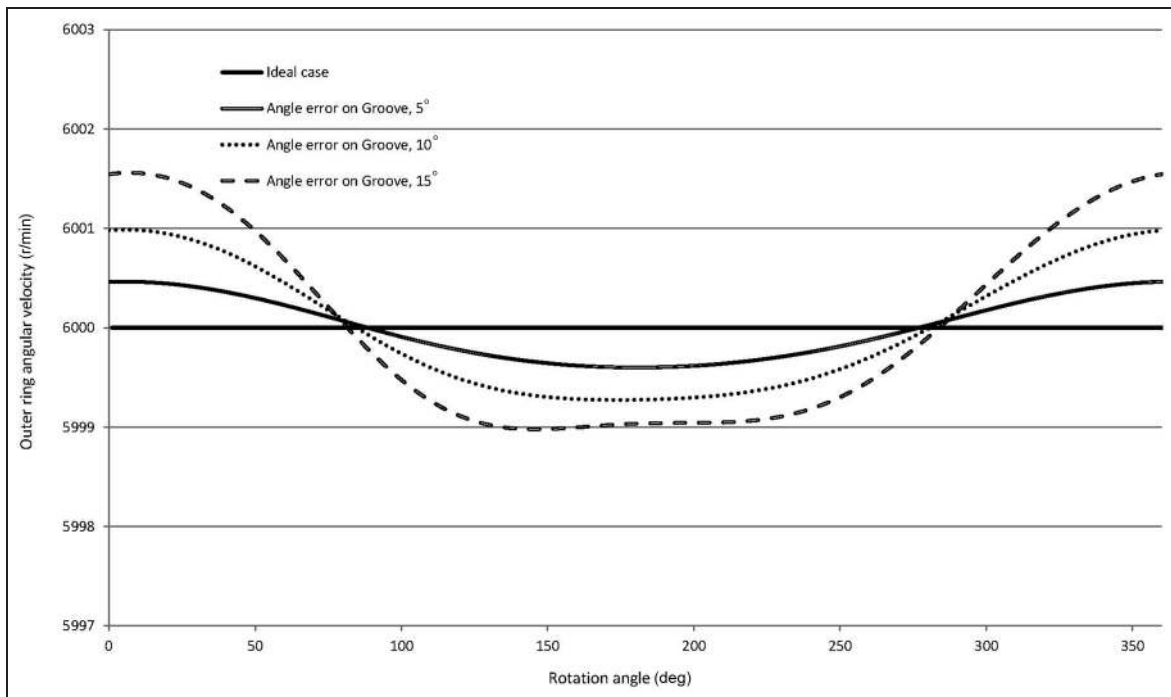


**Figure 12.** Kinematic irregularities in the angular velocity of the outer ring due to the angular error in the plane of the medial circle of the inner-ring groove.

homokineticity with irregularities in the transmission ratio with two contributions to the frequency. The main contribution consists of irregularities of the same frequency as that of the rotation (Figure 12). The secondary contribution consists of irregularities with smaller amplitudes but with a frequency which is the double

that of the rotation. This secondary contribution is more visible for a larger misalignment angle between the axes of the rings. The amplitudes of these irregularities are very similar to those caused by the first error. They increase (both main and secondary contributions) with increasing articulation angle between the inner

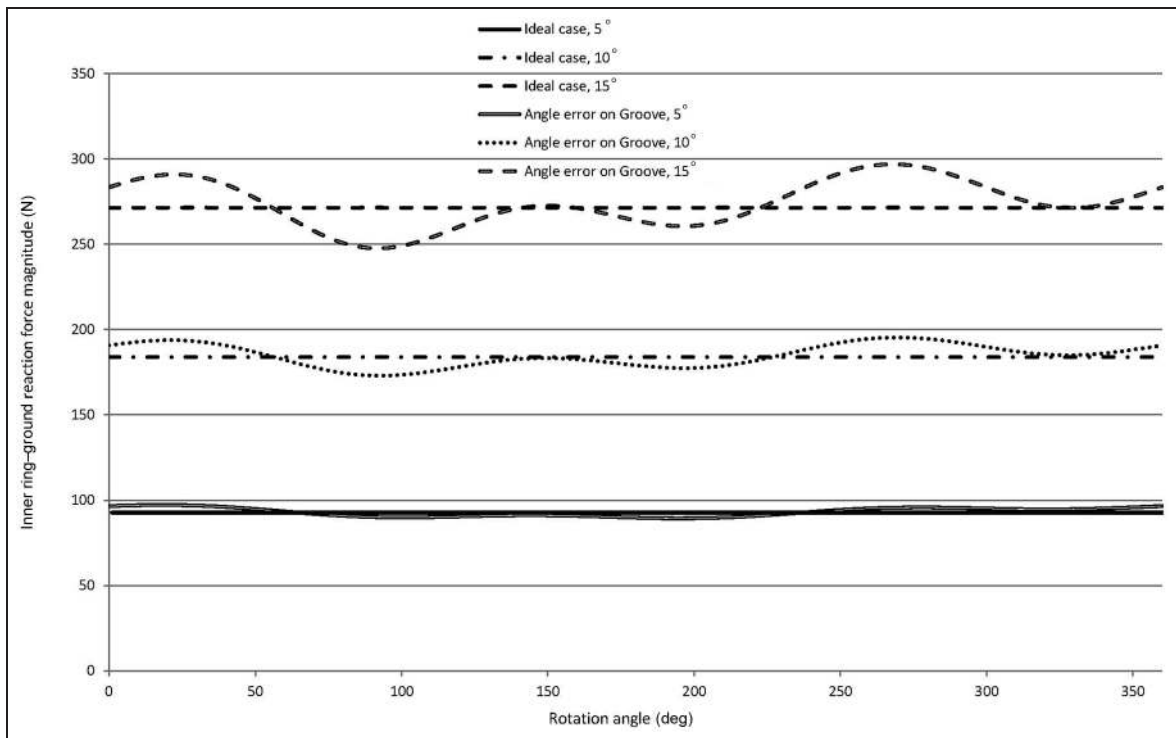


**Figure 13.** Dynamic irregularities in the inner-ring-ground reaction force due to the angular error in the plane of the medial circle of the inner-ring groove.

ring and the outer ring. At  $15^\circ$ , their combined effect reaches a maximum of 0.25%.

The reaction forces and moments acting on the revolute joints of both the inner ring and the outer ring are also irregular with two frequency contributions which have the same period and the same trend as those of the kinematic irregularities. Figures 13 and 14 present these irregularities for the inner ring. It can be observed that the mean value of the dynamic actions is the same as in the corresponding ideal case and that their amplitudes are smaller than those of the first error and the second error and increase with increasing articulation angle between the inner ring and the outer ring. Also, for this error, the irregularities in and the amplitudes of the outer ring are very similar, and they are omitted.

## Conclusions

In this paper, the influences of some relevant dimensional and geometrical errors on the kinematic performance and the dynamic performance of a Rzeppa ball joint were investigated. The study is based on the development of a dedicated multi-body 3D model and numerical simulations.

The model was revealed to be able to manage the occurrence of redundant constraints because of the use of specific spring connections between parts which describe the contact conditions with force relationships that are simpler than position constraints. The elastic characteristics of these spring elements were computed

using the Hertz theory in order to take into account the structural stiffnesses of the mating parts.

The modelling strategy produced a stable and precise integration of the equations of motion, allowing the irregularities to be demonstrated in an accurate way without numerical problems.

Three types of error were investigated: a geometrical error in the flatness of the active surface of the cage, a dimensional inaccuracy in the radius of one of the meridian grooves of the inner ring and an angular misalignment in the inclination of the plane in which one of the meridian circles of the inner groove is located.

The presence of each of these errors causes both kinematic irregularities and dynamic irregularities, the amplitudes of which increase with increasing articulation angle of the joint. The geometrical error of flatness in the active surface of the cage causes kinematic irregularities with the same frequency as that of the rotation and dynamic irregularities with a frequency which is double that of the rotation. The dimensional inaccuracy in the radius of one of the meridian grooves causes kinematic irregularities and dynamic irregularities with the same frequency as that of the rotation. The angular misalignment of one of the meridian circles of the inner groove causes more complex irregularities which involve a primary frequency equal to that of the rotation and a secondary frequency which is double that of the rotation and the effects of which become increasingly relevant with increasing angular misalignment of the joint.

The proposed investigation pointed out that, in the actual configuration with common precision



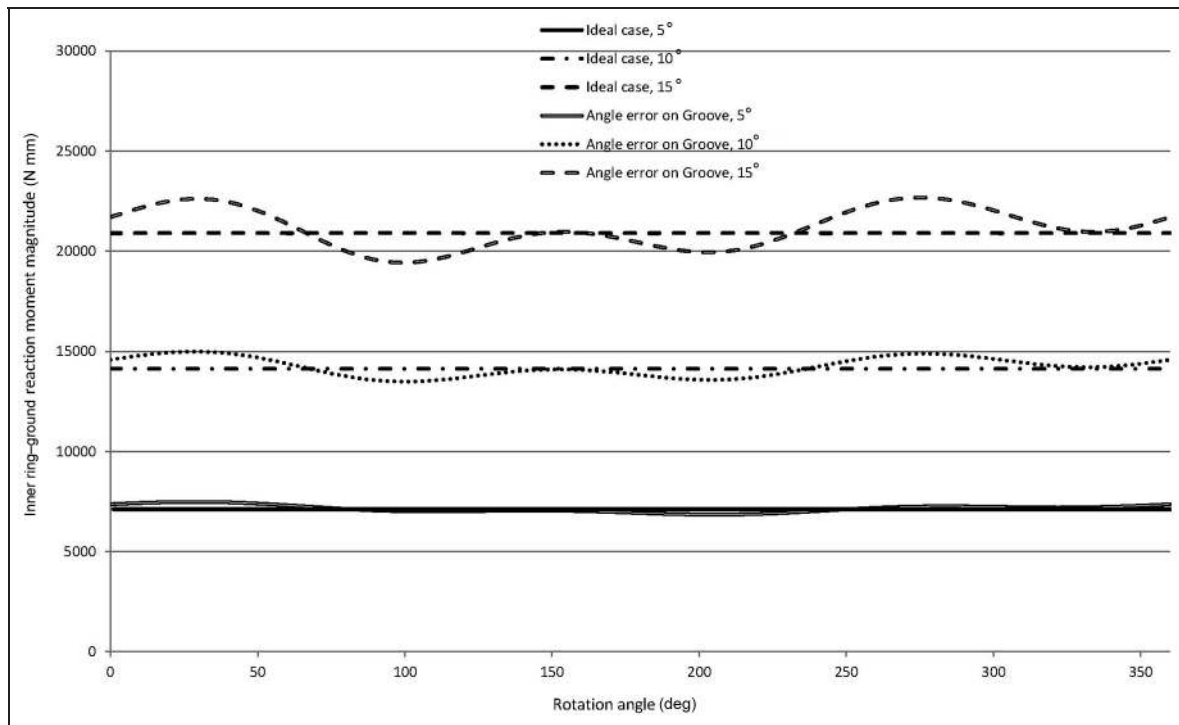


**Figure 14.** Dynamic irregularities in the inner-ring-ground reaction moment due to the angular error in the plane of the medial circle of the inner-ring groove.

manufacturing, the functioning of the Rzeppa joint produces irregularities which influence both the homokineticity characteristic and the presence of dynamic self-excitations. All these aspects should be taken into account in the choice of manufacturing precision, in the design of the joint and in the allocation of the tolerances when looking at the desired performances. Given a desired maximum amplitude of the irregularities, the values of the combined tolerances can be assessed by addressing specific simulations and comparing the values of the corresponding effects.

The same methodology of investigation and the same modelling techniques can be extended to other ball-type coupling joints.

#### Declaration of conflict of interest

The author declares that there is no conflict of interest.

#### Funding

This research received no specific grant from any funding agency in the public, commercial or not-for-profit sectors.

#### References

- Seherr-Thoss HChr, Schemelz F and Aucktor E. *Universal joint and driveshafts*. 2nd edition. Berlin: Springer, 2006.
- Wagner ER. *Universal joint and driveshaft design manual*. Warrendale, Pennsylvania: SAE International, 1991.
- Hunt KH. Constant-velocity shaft couplings: a general theory. *Trans ASME, J Engng Ind* 1979; 95: 445–464.
- Brutti C, Coglitore G and Valentini PP. Modelling of 3D revolute joint with clearance and contact stiffness. *Non-linear dynamics* 2011; 66: 531–548.
- Pezzuti E, Stefanelli R, Valentini PP and Vita L. Computer aided simulation and testing of spatial linkages with joint mechanical errors. *Int J Numer Meth Engng* 2006; 65: 1735–1748.
- Valentini PP. Tolerance allocation in spatial cam assembly for vehicle applications. *Int J Veh Systems Modeling Test* 2008; 3: 192–212.
- Hayama Y. NTN corporation: dynamic analysis of forces generated on inner parts of a double offset constant velocity universal joint (DOJ): non-friction analysis. SAE paper 2001-01-1161, 2001.
- Mariot J-P, K'nevez J-Y and Barbedette B. Tripod and ball joint automotive transmission kinetostatic model including friction. *Multibody System Dynamics* 2004; 11: 127–145.
- Kimata K, Nagatani H and Imoto M. Analysis of ball-type constant-velocity joints based on dynamics. *JSME Int J, Ser C* 2005; 47(2): 736–745.
- Serveto S, Mariot J-P and Diaby M. Secondary torque in automotive drive shaft ball joints: influence of geometry and friction. *Proc IMechE Part K: J Multi-body Dynamics* 2008; 222(3): 215–227.
- Pennestrì E and Valentini PP. Kinematic design and multibody analysis of the Rzeppa pilot-lever joint. *Proc IMechE Part K: J Multi-body Dynamics* 2008; 222(2): 135–142.
- Lim Y-H, Song M-E, Lee W-H et al. Multibody dynamics analysis of the driveshaft coupling of the ball

- and tripod types of constant velocity joints. *Multibody System Dynamics* 2009; 22: 145–162.
13. Fischer IS and Remington PM. Errors in constant-velocity shaft couplings. *Trans ASME, J Mech Des* 1994; 116: 204–209.
  14. Valentini PP and Pezzuti E. Effects of geometrical and dimensional errors on kinematics and dynamics of Tracta coupling. *J Theor Appl Mech* 2011; 49(1): 117–133.
  15. Cozzolini A, Pennestri E and Valentini PP. Virtual model of Rzeppa joint to assess performance in presence of geometric and dimensional tolerances. In: *ECCOMAS thematic conference on multibody dynamics*. The Institute of Aeronautics and Applied Mechanics (Warsaw University of Technology): Warsaw, Poland, 29 June–2 July 2009. (ISBN 978-83-7207-813-1)
  16. Myard FE. Contribution à la géométrie des systèmes articulés. *Bull Soc Math France* 1931; 59: 183–210.
  17. Young WC and Budynas RG. *Roark's formulas for stress and strain*. New York: McGraw-Hill, 2002.
  18. Haug EJ. *Computer-aided kinematics and dynamics of mechanical systems*, Vol 1. Boston, Massachusetts: Allyn and Bacon, 1988, pp. 48–104.
  19. Pennestri E, Mariti L, Valentini PP and Belfiore NP. Comparison of solution strategies for multibody dynamics equations. *Int J Numer Meth Engng* 2011; 88(7): 637–656.
  20. Gear CW. The numerical integration of ordinary differential equations. *Math Comput* 1967; 21: 146–156.
  21. ISO 2768-1 *General tolerances for linear and angular dimensions*. Geneva: International Organization for Standardization, 1989.